

Robust Detection and Estimation of Change-Points in a Time Series of Multivariate Images

Ammar Mian, Jean-Philippe Ovarlez, Guillaume Ginolhac, Abdourrahmane Atto

▶ **To cite this version:**

Ammar Mian, Jean-Philippe Ovarlez, Guillaume Ginolhac, Abdourrahmane Atto. Robust Detection and Estimation of Change-Points in a Time Series of Multivariate Images. EUSIPCO 2018, EURASIP, Sep 2018, Rome, Italy. 10.23919/eusipco.2018.8553285 . hal-01840793

HAL Id: hal-01840793

https://hal.univ-grenoble-alpes.fr/hal-01840793

Submitted on 16 Jul 2018

HAL is a multi-disciplinary open access archive for the deposit and dissemination of scientific research documents, whether they are published or not. The documents may come from teaching and research institutions in France or abroad, or from public or private research centers.

L'archive ouverte pluridisciplinaire **HAL**, est destinée au dépôt et à la diffusion de documents scientifiques de niveau recherche, publiés ou non, émanant des établissements d'enseignement et de recherche français ou étrangers, des laboratoires publics ou privés.

Robust Detection and Estimation of Change-Points in a Time Series of Multivariate Images

Ammar Mian*‡, Jean-Phillipe Ovarlez*†, Guillaume Ginolhac‡ and Abdourahmane Atto‡
*SONDRA, CentraleSupelec, FRANCE
†ONERA, DEMR/MATS, FRANCE
‡LISTIC, Université Savoie Mont-Blanc, FRANCE
Email: ammar.mian@centralesupelec.fr

***Abstract*—In this paper, we study the problem of detecting and estimating change-points in a time series of multivariate images. We extend existent works to take into account the heterogeneity of the dataset on a spatial neighbourhood. The classic complex Gaussian assumption of the data is replaced by a complex elliptically symmetric assumption. Then a robust statistics are derived using Generalised Likelihood Ratio Test (GLRT). These statistics are coupled to an estimation strategy for one or several changes. Performance of these robust statistics have been analyzed in simulation and compared to the one associated with standard multivariate normal assumption. When the data is heterogeneous, the detection and estimation strategy yields better results with the new statistics.**

***Index Terms*—Image Time Series; Robust Change Detection; multivariate Images; Complex Elliptically Symmetric;**

I. Introduction

Recent years have seen the increase of remotely sensed imaging systems and the number of satellite images available have grown significantly. Missions such as Sentinel-1 or TerraSAR-X deliver daily Synthetic Aperture Radar (SAR) images on a global scale. In this context, analysis of Image Time Series (ITS) for Change Detection (CD) purposes is a growing problematic. The information about change is useful for many applications such as environment monitoring or sea traffic surveillance.

New systems can provide multivariate images encompassing a certain kind of diversity. For example, Polarimetric radar sensors record the backscattering of the scene for different modes of polarization. For high-resolution Synthetic Aperture Radar (SAR) images, a diversity can be found in the spectral behaviour of the scatterers which may lead to vectors of great size [1]. In Hyperspectral images, the size of vectors is also large since the scene is imaged in numerous wavelengths. In those kind of images, the heterogeneity of the data is more apparent since the neighbourhood needed for the analysis is wider. The present paper considers the problem of change-point detection in ITS of such multivariate images.

CD literature is wide and many techniques have been investigated in the past years [2]. When considering pixel-based statistical techniques, classic schemes use a probability model from which a statistic of decision is derived. Works such as [3]–[5] have modeled the multivariate pixels as random Gaussian vectors and derived statistics of decision for bi-date CD as a test of covariance matrix equality. Recently, [6], [7] have considered and explored the problem of testing ITS. [8] proposed a method to estimate the point of change in such series using a Gaussian model.

However, when considering highly heterogeneous images such as high-resolution SAR images, it has been shown that the Gaussian assumption reflects poorly the distribution observed [9], [10]. In those contexts, the Complex Elliptically Symmetric (denoted $\mathbb{C}\mathcal{E}$) family of distributions has been proposed to model the dataset and solid results have been obtained in many applications. The Complex Angular Elliptical (denoted $\mathbb{C}\mathcal{AE}$) family, which is strongly linked to the $\mathbb{C}\mathcal{E}$ distributions [11], is of interest in the present paper. CD under non-Gaussian context has been explored in [12] where a similarity measure has been proposed under a bi-date framework. Recently, a Generalized Likelihood Ratio Test (GLRT) for similar distributions has been proposed by the present authors for bi-date CD in [13].

In this paper, we consider the problem of change-points detection in an ITS under $\mathbb{C}\mathcal{E}$ distributions assumption. We propose to adapt the methodology of [8] to this non-Gaussian context and derive the necessary statistics under the new formulation of the problem. We first remind the methodology of detection estimation and the statistics under Gaussian model. Then we derive the new robust statistics by means of GLRT. Finally, we test the algorithm of detection and estimation with the new statistics in simulation and conclude.

II. The Detection and Estimation Algorithm

A. Definitions and Problem

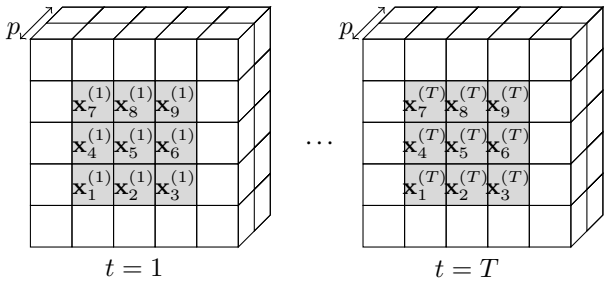


Fig. 1. Illustration of spatial neighbourhood ($N = 9$). The gray zone corresponds to the local observations at each date.

The work was supported by PHOENIX ANR-15-CE23-0012 grant of the French *National Agency of Research*.

Assume we have T multivariate images of the same scene at different dates. We define $\mathbb{T} = \{1 \dots T\}$, p the size of the vectors and N the number of local observations (pixels) $\{\mathbf{x}_k^{(t)}, k = 1 \dots N\}$ at a given date t.

On this local neighbourhood, we model the pixels as the realization of a random variable $\mathbf{x}$ with a probability density function (PDF) $p_{\mathbf{x}}(\mathbf{x}; \theta)$, where θ is a parameter of the PDF.

Under classic schemes, the Gaussian hypothesis has been privileged to model the data $p_{\mathbf{x}}(\mathbf{x}; \theta) = p_{\mathbf{x}}^{\mathbb{C}\mathcal{N}}(\mathbf{x}; \mathbf{\Sigma})$ where $\mathbf{\Sigma}$ is the covariance matrix of the data and sole parameter of the distribution since the mean is assumed to be null.

The problem considered presently is the following:
Consider a Time Series of random vectors $\mathbf{x}^{(t)} \sim p_{\mathbf{x}}(\mathbf{x}; \theta(t))$; given N independent observations $\{\mathbf{x}_k^{(t)}\}_{k=1\dots N}$, find all $t_C \in \mathbb{T} \backslash \{1\}$ so that $\theta(t_C - 1) \neq \theta(t_C)$. The number of total changes is unknown.

For simplification, the notation $\theta(t) \triangleq \theta_t$ will be used henceforth.

B. Detection problem: Binary Hypothesis testing

The first step consist in detecting the presence of a change in the time series. If the series is stationary, we assume that there is no change-point to be estimated. The so-called omnibus test scheme is intended to chose between the two following hypotheses:

$$\text{Let } (t_1, t_2) \in \mathbb{T}^2, \text{ so that } t_2 > t_1,$$
$$\begin{cases} \mathrm{H}_{0,\mathrm{omni}}^{t_1,t_2} : & \theta_{t_1} = \ldots = \theta_{t_2} = \theta_{t_1,t_2} \\ \mathrm{H}_{1,\mathrm{omni}}^{t_1,t_2} : & \exists (t,t') \in \{t_1, \ldots, t_2\}^2,\ \theta_t \neq \theta_{t'} \end{cases} \tag{1}$$

An appropriate statistic of the observations must be used to choose between the two hypotheses. Under Gaussian assumption ($\theta_t = \mathbf{\Sigma}_t$), several statistics have been derived for this problem [14]–[16]. A comparative study can be found in [7]. We remind here the statistic obtained by using the GLRT of the problem:

$$\hat{\Lambda}_{\mathbb{C}\mathcal{N},\mathrm{omni}}^{t_1,t_2} = \frac{\left| \sum_{t=t_1}^{t_2} \hat{\mathbf{\Sigma}}_t \right|^{(t_2-t_1)N}}{\prod_{t=t_1}^{t_2} \left| \hat{\mathbf{\Sigma}}_t \right|^N} \underset{\mathrm{H}_0}{\overset{\mathrm{H}_1}{\gtrless}} \lambda, \tag{2}$$

where $\forall t$, $\hat{\mathbf{\Sigma}}_t = 1/N \sum_{k=1}^N \left(\mathbf{x}_k^{(t)} \mathbf{x}_k^{(t)^H} \right)$ are the sample covariance matrices for each date, $|\bullet|$ is the determinant operator and λ is a threshold of detection.

C. Estimation Strategy

The scheme 1 allows to determine if there is one or more change. In case of a positive test, the location of the changes in the time series is to be estimated. To this end, successive bi-date detections scheme can be implemented:

$$\forall t \in \mathbb{T} \setminus \{1\},\ \begin{cases} \mathrm{H}_{0,\mathrm{bi-date}}^{t} : & \theta_{t-1} = \theta_t = \theta_{t-1,t} \\ \mathrm{H}_{1,\mathrm{bi-date}}^{t} : & \theta_{t-1} \neq \theta_t \end{cases} \tag{3}$$

However, this scheme exploits at most the data of two successive dates which is sub-optimal. An alternative scheme proposed in [8] is to consider successively the following marginal hypotheses:

$$\text{Consider } (t_1, t_2) \in \mathbb{T}^2, \text{ so that } t_2 > t_1,$$
$$\begin{cases} \mathrm{H}_{0,\mathrm{marg}}^{t_1,t_2} : \theta_{t_1} = \ldots = \theta_{t_2-1} = \theta_{t_1,t_2-1} \text{ and } \theta_{t_2-1} = \theta_{t_2} \\ \mathrm{H}_{1,\mathrm{marg}}^{t_1,t_2} : \theta_{t_1} = \ldots = \theta_{t_2-1} = \theta_{t_1,t_2-1} \text{ and } \theta_{t_2-1} \neq \theta_{t_2} \end{cases} \tag{4}$$

The GLRT for these hypotheses under $\mathbb{C}\mathcal{N}$ assumption has been derived as well:

$$\hat{\Lambda}_{\mathbb{C}\mathcal{N},\mathrm{marg}}^{t_1,t_2} = \frac{\left| \sum_{t=t_1}^{t_2} \hat{\mathbf{\Sigma}}_t \right|^{(t_2-t_1)N}}{\left| \hat{\mathbf{\Sigma}}_{t_2} \right|^N \left| \sum_{t=t_1}^{t_2-1} \hat{\mathbf{\Sigma}}_t \right|^{(t_2-t_1-1)N}} \underset{\mathrm{H}_0}{\overset{\mathrm{H}_1}{\gtrless}} \lambda. \tag{5}$$

D. The algorithm

Both detection and estimation can be done jointly using problems (1) and (4). [8] has proposed the following algorithm:

Algorithm 1 Change-Point Detection and Estimation

```
Initialize t_1 ← 1
while H_{1,omni}^{t_1,T} do                          ▷ Omnibus test
    Initialize r ← 1
    while H_{0,marg}^{t_1,t_1+r} do                  ▷ Successive marginal tests
        Update r ← r + 1
    end while
    Store t_1 + r − 1 as a change point
    Update t_1 ← t_1 + r
end while
```

The presented algorithm allows to detect several change points by first detecting a global change in the series and then refining the detection by iterating on the number of dates processed.

One key-point in the algorithm is the fact that statistics (2) and (5) have the Constant False Alarm (CFAR) property which means that their distribution is independent of the covariance matrix of the input data. In practice, this allows to select a threshold to guarantee a $\mathrm{P_{FA}}$ independently of the images of consideration. Hence, the strength of this method lies in the possibility to select a $\mathrm{P_{FA}}$ and the fact that the number of changes is not required to be known a priori.

When considering heterogenuous images, the Gaussian assumption is not realistic [10]. In this context, (2) and (5) are not optimal for detection. We propose in the next section to derive new statistics which are designed under more robust $\mathbb{C}\mathcal{E}$ model.

III. Extension to Non-Gaussian case

A. $\mathbb{C}\mathcal{E}$ and $\mathbb{C}\mathcal{A}\mathcal{E}$ distributions

A thorough description of $\mathbb{C}\mathcal{E}$ family can be found in [11]. We remind the PDF for any vector $\mathbf{x} \in \mathbb{C}^p$:

$$p_{\mathbf{x}}^{\mathbb{C}\mathcal{E}}(\mathbf{x}; \mathbf{\Sigma}, g) = \mathfrak{C}_{p,g} |\mathbf{\Sigma}|^{-1} g\left(\mathbf{x}^{\mathrm{H}} \mathbf{\Sigma}^{-1} \mathbf{x} \right), \tag{6}$$

where $\mathbf{\Sigma} \in \mathbb{S}_{\mathbb{H}}^p$ is a positive definite Hermitian matrix called the scatter matrix, and $g : \mathbb{R}^+ \to \mathbb{R}^+$ is a function called density generator that satisfies regularity conditions. $\mathfrak{C}_{p,g}$ is a normalization constraint ensuring that $\int_{\mathbb{C}^p} p_{\mathbf{x}}^{\mathbb{C}\mathcal{E}}(\mathbf{x})\mathrm{d}\mathbf{x} = 1$.

Under this assumption, we consider the problems (1), (3) and (4) with $\theta_t = \{g_t, \mathbf{\Sigma}_t\}$. However, the derivation is impossible when the density generators g_t are unknown.

To address this problem, we consider the self-normalized observations. Let $\mathbf{x} \sim \mathbb{C}\mathcal{E}(\mathbf{0}_p, g, \mathbf{\Sigma})$ and define $\mathbf{z} = \frac{\mathbf{x}}{\|\mathbf{x}\|_2}$. The self-normalized vector $\mathbf{z}$ is has a Complex Angular Elliptical distribution which is denoted as $\mathbb{C}\mathcal{AE}(\mathbf{0}_p, \mathbf{\Sigma}')$ [11], [17]. Since the normalized observations are systematically on the unit sphere of dimension p denoted $\mathbb{CS}^p$, they do not depend on the density generators and their PDF are fully known:

$$p_{\mathbf{z}}^{\mathbb{C}\mathcal{AE}}(\mathbf{z}; \mathbf{\Sigma}') = {\mathfrak{S}_p}^{-1}|\mathbf{\Sigma}'|^{-1}\left(\mathbf{z}^{\mathrm{H}}{\mathbf{\Sigma}'}^{-1}\mathbf{z}\right)^{-p}, \tag{7}$$

where $\mathfrak{S}_p = 2\pi^p/\Gamma(p)$ and Γ is the gamma function. As for the Gaussian case, the only parameter to consider is the scatter matrix. The derivation of statistics for problems (1) and (4) are done using $\theta_t = \{\mathbf{\Sigma}'_t\}$ and the PDF (7).

B. Omnibus Detection Test

Let us define, $\forall k,\ \forall t,\ \mathbf{z}_k^{(t)} = \mathbf{x}_k^{(t)}/\|\mathbf{x}_k^{(t)}\|_2$. To solve problem (1), we consider the following GLRT:

$$\hat{\Lambda}^{t_1,t_2}_{\mathbb{C}\mathcal{AE},\mathrm{omni}} = \frac{\max\limits_{\{\mathbf{\Sigma}_{t_1},\ldots,\mathbf{\Sigma}_{t_2}\}} \prod\limits_{t=t_1}^{t_2}\prod\limits_{k=1}^{N} p_{\mathbf{z}_k^{(t)}}^{\mathbb{C}\mathcal{AE}}(\mathbf{z}_k^{(t)}; \mathbf{\Sigma}_t)}{\max\limits_{\{\mathbf{\Sigma}_{t_1,t_2}\}} \prod\limits_{t=t_1}^{t_2}\prod\limits_{k=1}^{N} p_{\mathbf{z}_k^{(t)}}^{\mathbb{C}\mathcal{AE}}(\mathbf{z}_k^{(t)}; \mathbf{\Sigma}_{t_1,t_2})} \tag{8}$$

We treat both optimizations separately:

- First, let us consider the numerator. We have to maximize:

$$\begin{aligned}\mathcal{L} &= \prod_{t=t_1}^{t_2}\prod_{k=1}^{N} p_{\mathbf{z}_k^{(t)}}^{\mathbb{C}\mathcal{AE}}(\mathbf{z}_k^{(t)}; \mathbf{\Sigma}_t) \\ &\propto \prod_{t=t_1}^{t_2}\left(|\mathbf{\Sigma}_t|^{-N}\prod_{k=1}^{N}\left(\mathbf{z}_k^{(t)^{\mathrm{H}}}[\mathbf{\Sigma}_t]^{-1}\mathbf{z}_k^{(t)}\right)^{-p}\right).\end{aligned}$$

  The optimization is performed by solving separately for each $\{\mathbf{\Sigma}_t\}_{t\in\{t_1,\ldots,t_2\}}$. The obtained solution is the well-known Tyler's estimator:

$$\forall t,\ \hat{\mathbf{\Sigma}}_t^{\mathrm{TE}} = \frac{p}{N}\sum_{k=1}^{N}\frac{\mathbf{z}_k^{(t)}\mathbf{z}_k^{(t)^{\mathrm{H}}}}{\mathbf{z}_k^{(t)^{\mathrm{H}}}[\hat{\mathbf{\Sigma}}_t^{\mathrm{TE}}]^{-1}\mathbf{z}_k^{(t)}}. \tag{9}$$

- Now, let us consider the denominator. We have to maximize:

$$\begin{aligned}\mathcal{L} &= \prod_{t=t_1}^{t_2}\prod_{k=1}^{N} p_{\mathbf{z}_k^{(t)}}^{\mathbb{C}\mathcal{AE}}(\mathbf{z}_k^{(t)}; \mathbf{\Sigma}_{t_1,t_2}) \\ &\propto \prod_{t=t_1}^{t_2}\left(|\mathbf{\Sigma}_{t_1,t_2}|^{-N}\prod_{k=1}^{N}\left(\mathbf{z}_k^{(t)^{\mathrm{H}}}[\mathbf{\Sigma}_{t_1,t_2}]^{-1}\mathbf{z}_k^{(t)}\right)^{-p}\right).\end{aligned}$$

  Optimizing $\mathcal{L}$ towards $\mathbf{\Sigma}_{t_1,t_2}$ leads to:

$$\hat{\mathbf{\Sigma}}_{t_1,t_2}^{\mathrm{TE}} = \frac{p}{(t_2-t_1)N}\sum_{k=1}^{N}\sum_{t=t_1}^{t_2}\frac{\mathbf{z}_k^{(t)}\mathbf{z}_k^{(t)^{\mathrm{H}}}}{\mathbf{z}_k^{(t)^{\mathrm{H}}}[\hat{\mathbf{\Sigma}}_{t_1,t_2}^{\mathrm{TE}}]^{-1}\mathbf{z}_k^{(t)}}. \tag{10}$$

By replacing the estimates (9) and (10) in eq. (8) and we obtain the final statistic:

$$\hat{\Lambda}^{t_1,t_2}_{\mathbb{C}\mathcal{AE},\mathrm{omni}} = \frac{\left|\hat{\mathbf{\Sigma}}_{t_1,t_2}^{\mathrm{TE}}\right|^{(t_2-t_1)N}}{\prod\limits_{t=t_1}^{t_2}\left|\hat{\mathbf{\Sigma}}_t^{\mathrm{TE}}\right|^{N}}\prod_{t=t_1}^{t_2}\prod_{k=1}^{N}\frac{\left(\mathbf{z}_k^{(t)^{\mathrm{H}}}[\hat{\mathbf{\Sigma}}_{t_1,t_2}^{\mathrm{TE}}]^{-1}\mathbf{z}_k^{(t)}\right)^{p}}{\left(\mathbf{z}_k^{(t)^{\mathrm{H}}}[\hat{\mathbf{\Sigma}}_t^{\mathrm{TE}}]^{-1}\mathbf{z}_k^{(t)}\right)^{p}}. \tag{11}$$

C. Marginal Detection Test

The GLRT statistic for the problem (4) is given by:

$$\hat{\Lambda}^{t_1,t_2}_{\mathbb{C}\mathcal{AE},\mathrm{marg}} = \frac{\max\limits_{\{\mathbf{\Sigma}_{t_1,t_2-1},\mathbf{\Sigma}_{t_2}\}}\prod\limits_{k=1}^{N}\left(\prod\limits_{t=t_1}^{t_2-1}p_{\mathbf{z}_k^{(t)}}^{\mathbb{C}\mathcal{AE}}(\mathbf{z}_k^{(t)};\mathbf{\Sigma}_{t_1,t_2-1})\right)p_{\mathbf{z}_k^{(t_2)}}^{\mathbb{C}\mathcal{AE}}(\mathbf{z}_k^{(t_2)};\mathbf{\Sigma}_{t_2})}{\max\limits_{\{\mathbf{\Sigma}_{t_1,t_2}\}}\prod\limits_{k=1}^{N}\prod\limits_{t=t_1}^{t_2}p_{\mathbf{z}_k^{(t)}}^{\mathbb{C}\mathcal{AE}}(\mathbf{z}_k^{(t)};\mathbf{\Sigma}_{t_1,t_2})} \tag{12}$$

The derivation is similar to those of the omnibus test and yields:

$$\begin{aligned}\hat{\Lambda}^{t_1,t_2}_{\mathbb{C}\mathcal{AE},\mathrm{marg}} = {} & \frac{\left|\hat{\mathbf{\Sigma}}_{t_1,t_2}^{\mathrm{TE}}\right|^{(t_2-t_1)N}}{\left|\hat{\mathbf{\Sigma}}_{t_2}^{\mathrm{TE}}\right|^{N}\left|\hat{\mathbf{\Sigma}}_{t_1,t_2-1}^{\mathrm{TE}}\right|^{(t_2-t_1-1)N}}\times \\ & \prod_{k=1}^{N}\frac{\prod\limits_{t=t_1}^{t_2}\left(\mathbf{z}_k^{(t)^{\mathrm{H}}}[\hat{\mathbf{\Sigma}}_{t_1,t_2}^{\mathrm{TE}}]^{-1}\mathbf{z}_k^{(t)}\right)^{p}}{\left(\prod\limits_{t=t_1}^{t_2-1}\left(\mathbf{z}_k^{(t)^{\mathrm{H}}}[\hat{\mathbf{\Sigma}}_{t_1,t_2-1}^{\mathrm{TE}}]^{-1}\mathbf{z}_k^{(t)}\right)^{p}\right)\left(\mathbf{z}_k^{(t_2)^{\mathrm{H}}}[\hat{\mathbf{\Sigma}}_{t_2}^{\mathrm{TE}}]^{-1}\mathbf{z}_k^{(t_2)}\right)^{p}},\end{aligned} \tag{13}$$

where the estimates have been given in eq. (9) and (10).

D. Properties of the new statistics

As for (2) and (5) statistics, the new statistics (11) and (13) have the matrix CFAR property. The proof is omitted, but is straightforward from the one presented in [13]. The improvement comes from the fact that the new statistics are independent of the density generator which makes them more robust. This property is often referred as texture CFAR property.

The analytic distribution of both $\hat{\Lambda}^{t_1,t_2}_{\mathbb{C}\mathcal{AE},\mathrm{omni}}$ and $\hat{\Lambda}^{t_1,t_2}_{\mathbb{C}\mathcal{AE},\mathrm{marg}}$ under H_0 is unfortunately unknown. The problem will be considered in future developments. The selection of thresholds is done by obtaining the $\mathrm{P_{FA}}$ vs threshold of detection (a.k.a $P_{\mathrm{FA}} - \lambda$) curve by means of Monte-Carlo (M-C) Trials.

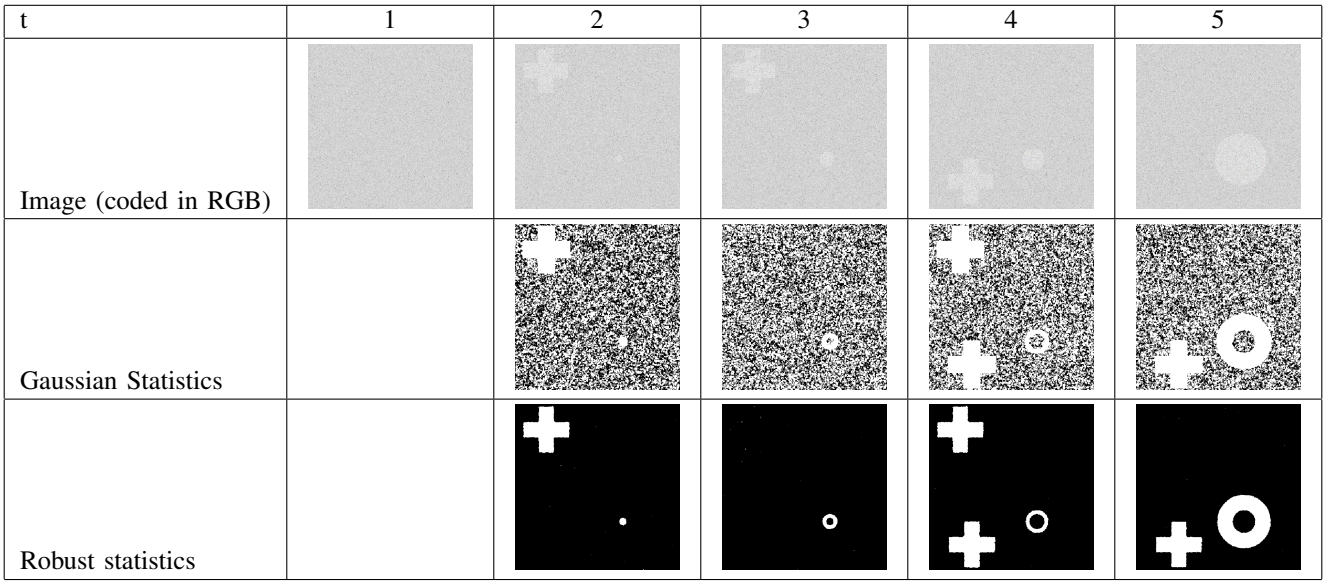


Fig. 2. Example of detection/estimation on synthetic images. $T = 5$, $p = 3$, $N = 25$, $\mathrm{P_{FA}} = 10^{-4}$. The background has parameters $\alpha = 0.3, \beta = 0.1, \rho = 0.99$. For the cross pattern: $\alpha = 0.3, \beta = 1, \mathrm{SNR} = 10$ dB, $\rho = 0.3$ and the circle pattern: $\alpha = 0.3, \beta = 1, \mathrm{SNR} = 10$ dB, $\rho = 0.2$.

TABLE I
SIMULATION-RELEVANT PARAMETERS

α, β	ρ_t	p	N	T
Shape and Scale for Γ-distribution	Coefficients for Toeplitz matrices	Size of vector	Number of observations	Number of Images

IV. SIMULATIONS

A. Description of simulation

The new statistics have been tested in simulation and compared to the Gaussian ones. Complex Compound Gaussian ($\mathbb{C}\mathcal{CG}$) random vectors, which is sub-family of the $\mathbb{C}\mathcal{E}$ distributions, have been considered. They are random vectors used are of the form $\mathbf{x} = \sqrt{\tau}\,\tilde{\mathbf{x}}$ where τ is a random monovariate variable with a given PDF, referred as the texture, and $\tilde{\mathbf{x}} \sim \mathbb{C}\mathcal{N}(\mathbf{0}_p, \mathbf{\Sigma})$. We choose $\tau \sim \Gamma(\alpha, \beta)$, where $\Gamma(\alpha, \beta)$ denotes the Gamma distribution with shape parameter α and scale parameter β.

The covariance matrices are chosen to be Toeplitz of the form $\mathbf{\Sigma}_t(m, n) = \rho_t^{|m-n|}$. ρ_t is the sole parameter governing the change over time.

Table I summarizes the relevant parameters for the simulations presented hereafter.

B. False alarm regulation

We first consider the regulation of false alarms for both robust omnibus and marginal detectors and compare them to the Gaussian one. To this end, synthetic images have been made where the background is a $\mathbb{C}\mathcal{CG}$ noise. A cross-shaped pattern appear, moves and disappear while a circle grows over time. The patterns correspond to realisation of $\mathbb{C}\mathcal{CG}$ vectors where the covariance matrix is different than for the background. The parameter β has been used to fix the Signal to Noise Ratio (SNR) of the patterns. The figure 2 present the different images of the series and the result of detection and estimation using algorithm 1 with both Gaussian and robust statistics. A white point on the resulting image t and position (x, y) correspond to a point that has been detected as a change in the time series at position (x, y) and estimated to be at time t. The thresholds have been chosen to guarantee a $\mathrm{P_{FA}} = 10^{-4}$ using theoretical relationship for Gaussian statistics (given in [8] for example) while M-C trials have been used for the robust one. Results show that for Gaussian statistics, the $\mathrm{P_{FA}}$ chosen is not respected: a significant number of false alarms are present. Results with robust statistics show that the number of false alarms is greatly reduced. This result is expected since the Gaussian statistics do not account for the nature of the data.

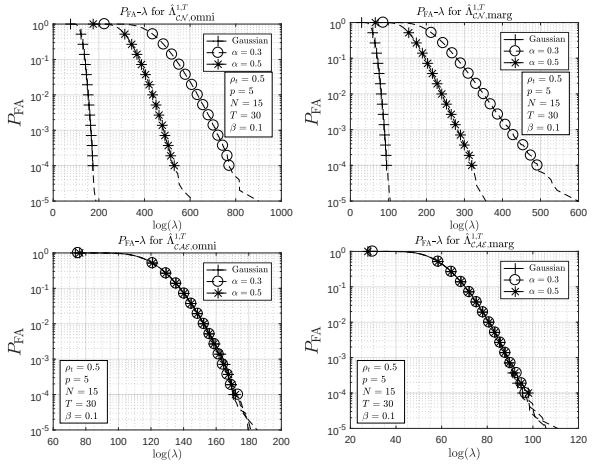


Fig. 3. $\mathrm{P_{FA}} - \lambda$ relationships for several parameters of the $\mathbb{C}\mathcal{CG}$ distribution.

Next, $\mathrm{P_{FA}} - \lambda$ curves have been computed, by means of M-C trials, at Figure 3. The figure show the curves for Gaussian

model and $\mathbb{C}\mathcal{CG}$ one with several parameters for the texture. We observe that the curves are not the same for the Gaussian statistics while for robust statistics, the curves are the same. This result confirms the texture CFAR property of the robust statistics.

C. Probability of detection

To compare the performance of detection of Gaussian and robust schemes, we choose to compute the probability of detection at the good date P_D, through means of M-C trials, on a simple situation where there is only one change at a date t_C. Before the change, we choose $\rho_{t<t_C} = 0.01$ and after the change several values have been used. Both Gaussian and $\mathbb{C}\mathcal{CG}$ models have been simulated and the expetimental thresholds, for the given noise, have been chosen for the P_{FA} selected. The Bartlett distance [18] on covariance matrices has been used as a measure of the amplitude of the change:

$$d_{\mathcal{B}}(\mathbf{\Sigma}_1, \mathbf{\Sigma}_2) = \log(\frac{|\mathbf{\Sigma}_1 + \mathbf{\Sigma}_2|^2}{|\mathbf{\Sigma}_1|\ |\mathbf{\Sigma}_2|}) - 2p\log(2). \tag{14}$$

The results, presented at Figure 4, have also been compared to the bi-date scheme presented at eq. (3).

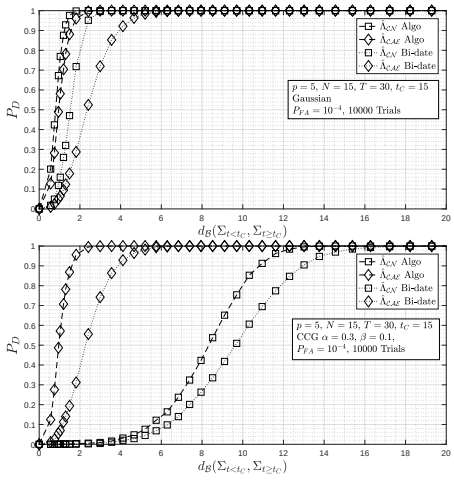


Fig. 4. Probability of detection versus Bartlett distance.

When the data follows a Gaussian distribution, we notice that the performance is lower for the robust statistics in comparison to the Gaussian ones. The plot also shows that even for a single change, the algorithm 1 performs better than the bi-date one. When the data follows a $\mathbb{C}\mathcal{CG}$ distribution, the performances are the same for the robust statistics while the performances strongly decrease with Gaussian statistics.

V. Conclusion

The present paper has studied the problem of change-point detection in a series of multivariate images under non-Gaussian assumption. An extension of [8] to $\mathbb{C}\mathcal{E}$ family has been proposed and studied in simulation. The proposed detector yields a robust behaviour for a large family of distributions. Future works concern the performance analysis of this methodology on real experimental data such as Sentinel-1 SAR images.

References

[1] J. P. Ovarlez, G. Ginolhac, and A. M. Atto, "Multivariate linear time-frequency modeling and adaptive robust target detection in highly textured monovariate sar image," in *2017 IEEE International Conference on Acoustics, Speech and Signal Processing (ICASSP)*, March 2017, pp. 4029–4033.

[2] M. Hussain, D. Chen, A. Cheng, H. Wei, and D. Stanley, "Change detection from remotely sensed images: From pixel-based to object-based approaches," {*ISPRS*} *Journal of Photogrammetry and Remote Sensing*, vol. 80, pp. 91 – 106, 2013. [Online]. Available: http://www.sciencedirect.com/science/article/pii/S0924271613000804

[3] L. M. Novak, "Coherent change detection for multi-polarization SAR," in *Conference Record of the Thirty-Ninth Asilomar Conference onSignals, Systems and Computers, 2005.*, Oct 2005, pp. 568–573.

[4] V. Carotenuto, A. D. Maio, C. Clemente, and J. Soraghan, "Unstructured versus structured GLRT for multipolarization SAR change detection," *IEEE Geoscience and Remote Sensing Letters*, vol. 12, no. 8, pp. 1665–1669, Aug 2015.

[5] K. Conradsen, A. A. Nielsen, J. Schou, and H. Skriver, "Change detection in polarimetric SAR data and the complex Wishart distribution," in *IGARSS 2001. Scanning the Present and Resolving the Future. Proceedings. IEEE 2001 International Geoscience and Remote Sensing Symposium (Cat. No.01CH37217)*, vol. 6, 2001, pp. 2628–2630 vol.6.

[6] A. A. Nielsen, K. Conradsen, and H. Skriver, "Omnibus test for change detection in a time sequence of polarimetric SAR data," in *2016 IEEE International Geoscience and Remote Sensing Symposium (IGARSS)*, July 2016, pp. 3398–3401.

[7] D. Ciuonzo, V. Carotenuto, and A. D. Maio, "On multiple covariance equality testing with application to SAR change detection," *IEEE Transactions on Signal Processing*, vol. 65, no. 19, pp. 5078–5091, Oct 2017.

[8] K. Conradsen, A. A. Nielsen, and H. Skriver, "Determining the points of change in time series of polarimetric sar data," *IEEE Transactions on Geoscience and Remote Sensing*, vol. 54, no. 5, pp. 3007–3024, May 2016.

[9] E. Ollila, D. E. Tyler, V. Koivunen, and H. V. Poor, "Compound-Gaussian clutter modeling with an inverse Gaussian texture distribution," *IEEE Signal Processing Letters*, vol. 19, no. 12, pp. 876–879, Dec 2012.

[10] M. S. Greco and F. Gini, "Statistical analysis of high-resolution SAR ground clutter data," *IEEE Transactions on Geoscience and Remote Sensing*, vol. 45, no. 3, pp. 566–575, March 2007.

[11] E. Ollila, D. E. Tyler, V. Koivunen, and H. V. Poor, "Complex elliptically symmetric distributions: Survey, new results and applications," *IEEE Transactions on Signal Processing*, vol. 60, no. 11, pp. 5597–5625, Nov 2012.

[12] M. Liu, H. Zhang, C. Wang, and F. Wu, "Change detection of multilook polarimetric SAR images using heterogeneous clutter models," *IEEE Transactions on Geoscience and Remote Sensing*, vol. 52, no. 12, pp. 7483–7494, Dec 2014.

[13] A. Mian, J.-P. Ovarlez, G. Ginolhac, and A. M. Atto, "A robust change detector for highly heterogeneous images." 2018 IEEE International Conference on Acoustics, Speech and Signal Processing, 2018, p. to appear.

[14] H. Nagao, "On some test criteria for covariance matrix," *Ann. Statist.*, vol. 1, no. 4, pp. 700–709, 07 1973. [Online]. Available: https://doi.org/10.1214/aos/1176342464

[15] J. R. Schott, "Some tests for the equality of covariance matrices," *Journal of Statistical Planning and Inference*, vol. 94, no. 1, pp. 25 – 36, 2001. [Online]. Available: http://www.sciencedirect.com/science/article/pii/S0378375800002093

[16] M. Hallin and D. Paindaveine, "Optimal tests for homogeneity of covariance, scale, and shape," *Journal of Multivariate Analysis*, vol. 100, no. 3, pp. 422 – 444, 2009. [Online]. Available: http://www.sciencedirect.com/science/article/pii/S0047259X08001474

[17] I. Soloveychik and A. Wiesel, "Tyler's covariance matrix estimator in elliptical models with convex structure," *IEEE Transactions on Signal Processing*, vol. 62, no. 20, pp. 5251–5259, Oct 2014.

[18] A. C. Frery, A. D. C. Nascimento, and R. J. Cintra, "Analytic Expressions for Stochastic Distances Between Relaxed Complex Wishart Distributions," *IEEE Transactions on Geoscience and Remote Sensing*, vol. 52, pp. 1213–1226, Feb. 2014.